

RSC Advances



This is an *Accepted Manuscript*, which has been through the Royal Society of Chemistry peer review process and has been accepted for publication.

Accepted Manuscripts are published online shortly after acceptance, before technical editing, formatting and proof reading. Using this free service, authors can make their results available to the community, in citable form, before we publish the edited article. This *Accepted Manuscript* will be replaced by the edited, formatted and paginated article as soon as this is available.

You can find more information about *Accepted Manuscripts* in the [Information for Authors](#).

Please note that technical editing may introduce minor changes to the text and/or graphics, which may alter content. The journal's standard [Terms & Conditions](#) and the [Ethical guidelines](#) still apply. In no event shall the Royal Society of Chemistry be held responsible for any errors or omissions in this *Accepted Manuscript* or any consequences arising from the use of any information it contains.

ARTICLE

Preparation of PDMS Ultrathin Films and Patterned Surface Modification with Cellulose

Cite this: DOI: 10.1039/x0xx00000x

Matej Bračič,^{a,e*} Tamilselvan Mohan,^{b,*} Rupert Kargl,^a Thomas Griesser,^c Silvo Hribernik,^a Stefan Köstler,^d Karin Stana-Kleinschek,^b and Lidija Fras-Zemljič^aReceived 00th January 2012,
Accepted 00th January 2012

DOI: 10.1039/x0xx00000x

www.rsc.org/

In this investigation, polydimethylsiloxane (PDMS) ultrathin films are prepared on a variety of solid surfaces by a simple and fast spin coating method, and patterned with the natural biopolymer cellulose via lithographic methods. Two surface patterning methods are developed to create coatings of hydrophilic cellulose, regenerated from trimethylsilyl cellulose (TMSC) on the PDMS thin films. In method 1, spin coated TMSC films on PDMS are covered with a lithographic mask and exposed to vapors of hydrochloric acid, which results in spatially separated cellulose pads surrounded by TMSC. Subsequent selective dissolution of TMSC with organic solvents results in a direct anchoring of cellulose pads on the PDMS. In method 2, PDMS thin films covered with a lithographic mask are exposed to UV/ozone, spray coated with TMSC and regenerated to cellulose. The conversion of hydrophobic TMSC into hydrophilic cellulose coatings is confirmed by wettability and fluorescence measurements. The developed structures are highly transparent and stable in aqueous solutions (pH 3-9) and organic solvents. The surface properties of the polymer films are characterized using a quartz crystal microbalance with dissipation (QCM-D), ellipsometry, X-ray photoelectron spectroscopy (XPS), atomic force microscope (AFM), contact angle and streaming potential measurements.

1. Introduction

Polydimethylsiloxane (PDMS) is an often used material in microfluidics,¹ soft-lithography and optical waveguides due to its excellent biocompatibility, chemical inertness, high elasticity and transparent nature.^{2,3} Despite its advantages, the native hydrophobic surface of PDMS is not ideal for applications like cell growth, blood compatibility and biomedical implants without a proper surface modification, since it shows a strong non-specific binding/interaction towards proteins, cells, and antibodies. In this context, the knowledge of the surface properties such as surface free energy (SFE), surface chemical composition and surface charge of native and surface modified PDMS is crucial. To obtain better control and understanding on the interaction of biomolecules with surfaces (*e.g.* ionic strengths, pH, etc.) thin polymer films are often used. In this case, a comprehensive characterization of the substrates can be performed and all modern surface analytical methods can be employed. While knowledge already exists for the manufacturing of casted PDMS, the preparation of thin films with a layer thickness below 30 nm via spin coating is still a challenging task.^{4,5} A simple procedure that allows a fast preparation of PDMS thin films with

controlled physiochemical properties is therefore demanded. For many applications, a combination of 2D patterning of surfaces and a site-selective immobilization of biomolecules is often preferred. In order to define reaction or detection zones in bio-analytical devices or cell growth scaffolds, micro- or nanostructuring is regularly applied.⁶⁻¹⁰ For that purpose several surface patterning methods such as photolithography,¹¹ UV/ozone^{8,12,13} or plasma treatment^{11,14} in combination with soft-lithography^{9,15} have been developed. One particular method is UV/ozone lithography. This method relies on the exposure of mask-covered PDMS surfaces to UV/ozone, which renders the surfaces hydrophilic.^{15,16} However, the UV treated surfaces are unstable and regain their hydrophobicity with time.¹⁷ This hydrophobic recovery is a well-known problem in polymer surface modification and especially pronounced for PDMS due to its low glass transition temperature.¹⁸ Alternatively, the exposed areas can be decorated permanently with hydrophilic polymers such as polyethylene oxide, block copolymers, mucin, poly(L-lysine) (PLL)-g-PEG.¹⁹ Using this approaches, micro- or nano-patterned deposition of polymers exhibiting antifouling behavior can be obtained and utilized for the above mentioned applications. Compared to many synthetic polymers, cellulose, the most abundant biopolymer on

earth, has desirable properties such as high hydrophilicity, low toxicity, high biocompatibility and low fouling properties.²⁰⁻²² To prepare coatings of cellulose, the cellulose derivative, trimethylsilyl cellulose (TMSC), soluble in organic solvents, can be coated on PDMS surface and converted into pure cellulose by vapor-phase acid treatment.^{23,24}

The aim of this work was therefore to establish a fast and simple procedure for the manufacturing of nanometric PDMS thin films with defined physicochemical properties and to spatially functionalize these surfaces with hydrophilic cellulose coatings. PDMS films with different layer thicknesses were prepared on different solid substrates and their surface properties such as wettability, surface free energy (SFE), chemical composition, morphology and streaming potential were analyzed. Subsequently, PDMS films were coated with TMSC, and structured by UV/ozone treatments and lithographic techniques. The stability of the functional films was also tested.

2. Experimental Section

2.1 Materials

Sylgard 184 Silicone elastomer Kit was purchased from Dow Corning, USA. Silicon wafers covered with silicon oxide with a thickness of 100 nm and a surface orientation of 100 were purchased from Silchem, Freiburg, Germany. Trimethylsilyl cellulose (TMSC) with a degree of substitution (DS_{Si}) of 2.8, purchased from TITK Rudolstadt, Germany, and produced by the silylation of Avicel was used as starting material for the cellulose film preparation.²⁵ Tetramethylrhodamine isothiocyanate (TRITC) was purchased from Sigma-Aldrich, Austria and used as received. Quartz crystal microbalance (QCM) crystals coated with a gold layer (QX303) and silicon dioxide (SiO_2 , QSX-301) were purchased from LOT-Oriel, Germany. Microscope glass slides ($25 \times 75 \text{ mm}^2$) were purchased from Roth, Austria. For contact angle measurements four different liquids were used: Milli-Q water ($>18 \text{ m}\Omega \text{ cm}$) from a Milli-Q-water system (Millipore, USA), diiodomethane (Sigma-Aldrich, 99%), formamide (Sigma, 99%), and ethylene glycol (Sigma-Aldrich, 99.8%), all of analytical grade. Toluene (99.9%), tetrahydrofuran (THF, $\geq 99.9\%$); sodium chloride ($\geq 99.5\%$) and potassium chloride ($\geq 99.0\%$) were purchased from Sigma-Aldrich, Austria and used as received.

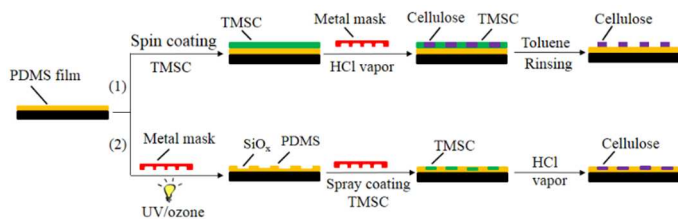
2.2. Substrate cleaning and PDMS thin film preparation

For spin coating of PDMS, three different substrates were used. Silicon wafers were cut into pieces of $2 \times 2 \text{ cm}^2$, rinsed with ethanol, rinsed with pure water and immersed into a "piranha" solution (H_2SO_4 (98%)/ H_2O_2 (30%), 70:30 (v/v)) for 15 min, stored in Milli-Q water for at least 30 min and blow dried with nitrogen gas. QCM-D sensors were soaked into a mixture of H_2O/H_2O_2 (30 wt. %)/ NH_4OH (25 wt. %) (5:1:1; v/v/v) for 10 min at $70 \text{ }^\circ\text{C}$, immersed in a "piranha" solution for 40 s, rinsed with pure water and finally blow dried with nitrogen gas. Glass slides ($25 \times 75 \text{ mm}^2$) were rinsed with ethanol, immersed in MQ-water for 30 min, in piranha solution

for 60 min, again in MQ-water for 30 min, rinsed with MQ-water and finally blow dried with N_2 gas. Silicone elastomer (10:1 (w/w)), mixture of base and curing agent) was used for the manufacturing of PDMS thin films. A stock solution of 10 % (w/w) PDMS was prepared by dissolving the elastomer in toluene or in tetrahydrofuran (THF) and shaking for 12 hours. PDMS with concentrations ranging from 0.1 – 0.7 % (w/w) were prepared from the stock solution by diluting it with toluene or with THF and shaking for 12 hours. 100 μl of PDMS solution was deposited on a cleaned static substrate (Au and SiO_2) and then rotated at a spinning speed of 5000 revolutions per minute (rpm) and an acceleration of 2500 rpm s^{-1} for 60 s. For coatings on glass slides, 2 ml of PDMS solution (0.5 %, w/w) were used and spin coated as above. The coated films were subsequently cured in a vacuum oven at $80 \text{ }^\circ\text{C}$ for 12 hours.

2.3. Structuring of PDMS surfaces with cellulose/TMSC coatings and stability test

Two methods were used to spatially functionalize PDMS surfaces with cellulose (Scheme 1). In method 1, 2 ml of TMSC solution (1 % (w/v), dissolved in toluene by heating to $60 \text{ }^\circ\text{C}$ followed by cooling down to room temperature, filtered through a $5 \mu\text{m}$ PTFE filter) was deposited on the PDMS slide ($25 \times 75 \text{ mm}^2$), rotated for 60 s at a spinning speed of 4000 rpm and an acceleration of 2500 rpm s^{-1} . For the spatial structuring, the TMSC coated PDMS slides were covered with an aluminum mask ($75 \times 25 \text{ mm}^2$, thickness: 1 mm) bearing 16 squared holes ($5 \times 5 \text{ mm}^2$) and placed into a 1000 ml desiccator containing 300 ml of 10 wt. % HCl. The slides were exposed to vapors of HCl for 15 min. The conversion of TMSC into pure cellulose is designated as 'regeneration' in this work. The unexposed areas were rinsed with toluene for 1 min, with pure water for 20 min and blow dried with nitrogen gas. The details of the spin coating and regeneration procedure are reported elsewhere.^{26, 27} In method 2, the same aluminum mask was pressed against the PDMS coated glass slides and exposed to UV-light (PSD Pro Series Digital UV Ozone System from Novascan (USA) containing a mercury light source emitting at 185 and 254 nm) for 60 min under pure oxygen at $50 \text{ }^\circ\text{C}$. Following this, a TMSC (1 %, w/v) solution was sprayed on the UV/ozone treated areas using an air brush while covering the remaining areas with the aluminum mask. An air brush with a nozzle diameter of 0.635 mm (Roth, Austria) was connected to a compressed nitrogen source (30 psi) and used to spray coat the TMSC solution. The spray coated slides were then dried in air at room temperature for 10 min. The TMSC was converted into cellulose as described above. All structured slides were subsequently stained with TRITC. 25 μl of TRITC ($0.25 \mu\text{g ml}^{-1}$) dissolved in pure water was deposited on the regenerated cellulose pads and incubated for 30 min. After this step, the slides were extensively rinsed with pure water and blow dried with nitrogen gas. To test the stability, the structured slides were rinsed with buffer solution of different pH values (4, 7, and 9) for 30 min, rinsed with pure water (10 min) and blow dried with nitrogen gas.



Scheme. 1 Patterned deposition of cellulose from TMSC on PDMS surfaces via the combination of UV/ozone and lithographic techniques. Method 1) Spin coating and spatial regeneration of TMSC to cellulose. Method 2) UV/ozone treatment followed by spray coating and spatial regeneration of TMSC to cellulose.

2.4. Analytical methods

Ellipsometry: Film thickness was measured by ellipsometry using an auto-nulling imaging ellipsometer Nanofilm ep3se (Accurion, Germany). The samples were illuminated with a laser light at a wavelength of $\lambda = 658$ nm and the measurements were performed using a range of incidence angles, varying from 42° to 55° . A refractive index of 1.4 was used for calculating the PDMS film thickness.²⁸ Detailed information about the EP4model can be found elsewhere.²⁹ **X-ray photoelectron spectroscopy (XPS):** XPS spectra were recorded with a monochromatic K-Alpha spectrometer equipped with an Al X-ray source (1486.6eV) operating with a base pressure in the range of 10^{-8} to 10^{-10} mbar. Survey scans were acquired with a pass energy of 100 eV and a step size of 1.0 eV. All spectra were normalized to the Au $4f_{7/2}$ peak. The average chemical composition was calculated from wide scan spectra in two different locations on each surface. All analyses were performed at room temperature. **Contact angle and surface energy determination:** Contact angle measurements and surface free energy (SFE) calculations were performed using a goniometer system OCA15+ (Dataphysics, Germany). Static contact angle (SCA) measurements were carried out using four different liquids: Milli-Q water, diiodomethane, formamide, and ethylene glycol. All measurements were carried out at ambient temperature with a drop volume of 3 μ l. Each SCA value was the average of at least five drops of liquid per surface. The total SFE (γ_s^{TOT}) was calculated using the acid base approach of van Oss and Good. The advancing and receding contact angles were obtained by increasing and decreasing (0.1μ l s^{-1}) the volume of a small water droplet (originally 10 μ l) with a thin needle. At least three reproducible measurements from duplicate samples were performed. More detailed information on the use of the equations and the surface tension components of the liquids used for SCA measurements can be found elsewhere.²³ **Zeta potential:** The streaming potential measurements were carried out using a homebuilt EKA-Oszi apparatus, which creates an oscillator flow of electrolyte through and alongside the flat sample. Each measurement of PDMS coated glass slides was carried out in the pH range of 2.4 to 9.7 in 1 mM KCl solution and repeated 3 times. A detailed description of the instrument and the working principle can be found elsewhere.³⁰ **Quartz crystal microbalance with dissipation (QCM-D):** A QCM-D device (model E4 from Q-Sense, Gothenburg,

Sweden) was used to determine the film thickness, mass and stability of the PDMS coated surfaces. A description of the QCM-D technique, layer thickness calculation and stability of the coated PDMS film can be found in ESI†. **Optical light microscopy:** The morphology of the spin coated films was observed with an Axiotech 25 HD light optical microscope (Carl Zeiss Jena GmbH, Germany) at 50x magnification. The images were recorded with a high resolution AxioCam MRc (D) camera attached to the microscope and processed using the KS 300 Rel.3.0 “true color analysis” imaging software. **Atomic force microscopy (AFM):** Topographical features of the surfaces were characterized by AFM in tapping mode with an Agilent 5500 AFM multimode scanning probe microscope (Digital Instruments, Santa Barbara, CA). The images were scanned using silicon cantilevers (ATEC-NC, Nanosensors, Germany) with a resonance frequency of 210-490 kHz and a force constant of 12-110 N/m. All measurements were performed at ambient temperature in air. **Fluorescence Scanning:** Microarray fluorescence scanning was performed on a microarray scanner DNAscope LM+ from GeneFocus, USA, with green excitation (523 nm) and red emission at a 5 μ m resolution and at PMT gain of 55%. The images were colored red by the software.

3. Result and Discussion

3.1. Film characterization: structure, thickness, topography and wettability

The Sauerbrey mass and thickness of the PDMS films as a function of the polymer concentration is shown in Fig.1. Owing to the fact that the Sauerbrey equation can be applied to dry and rigid films, we are able to calculate the mass of the coated films directly by using the Sauerbrey equation (see ESI†). In such cases the change in dissipation (ΔD_3) should be below 2×10^{-6} . In our case, the observed changes in dissipation for all films were $0.2 \pm 0.01 \times 10^{-6}$. As can be seen in Fig. 1, the Sauerbrey mass and therefore the related thickness both increase linearly from 0.1 to 0.5 (w/w). Low concentrations (0.1 %, w/w) lead to films with a mass of $0.3 \pm 0.02 \mu$ g cm^{-2} (3.8 ± 0.8 nm). Whereas higher concentrations (0.7 %, w/w) give films with $3 \pm 0.2 \mu$ g cm^{-2} (27 ± 1.1 nm). This clearly shows that the film thickness can be accurately adjusted by the polymer concentration during spin coating.

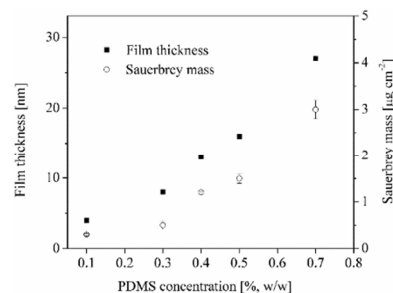


Fig.1 Comparison of film mass and thickness as a function of the PDMS concentration.

Additionally, the ellipsometric and QCM-D film thickness are compared and correlated with the silicon content as a function of PDMS concentration (see ESI, Fig. S1†). The values determined with these complementary methods correlate well, which clearly shows that QCM-D is reliable for the indirect thickness measurement of solid PDMS thin films. The XPS high resolution spectra showed a peak at 100.9 eV (Si2p) for films coated from all concentrations which can be attributed to O–Si–C bonds in the siloxane.³¹ For concentrations of 0.5 % (w/w) the silicon content of the film reaches the theoretical value (Table 1) comparable with published results.³¹ For the higher concentrations (0.7 % w/w) the Si content is above this value which can be explained by the morphological inhomogeneity as shown in section 3.3. For thinner films, the silicon content is below 20 at. % owing to the contribution of the gold signal from the substrate. This discrepancy in silicon content can be explained by the emergence of other atoms, namely Au, from the underlying QCM gold coated surface. The appearance of the Au signal in the spectrum is consistent with the sampling depth of the XPS instrument at normal incidence, which is typically around 10 nm.³¹ At higher thickness, the underlying gold layer is no longer visible and a closed PDMS film can be assumed. By varying the PDMS concentration one can successfully control the thickness of the coated PDMS films and well defined model surfaces which represent pure PDMS are obtained.

Table 1. Atomic compositions obtained from XPS survey spectra for PDMS films manufactured from different concentration. All concentrations are given in w/w.

	Atomic percentage (%)			
	C	O	Si	Au
Theoretical	50	25	25	-
PDMS (0.1 %)	43.2 ± 1.2	20.6 ± 1.3	16.4 ± 0.2	19.8 ± 2.3
PDMS (0.3 %)	48.1 ± 1.3	24.9 ± 0.2	20.5 ± 0.5	6.6 ± 1.1
PDMS (0.4 %)	48.3 ± 1.2	24.3 ± 0.8	22.7 ± 0.7	4.7 ± 0.4
PDMS (0.5 %)	50.0 ± 0.2	25.0 ± 0.1	25.0 ± 0.3	-
PDMS (0.7 %)	48.2 ± 1.8	23.7 ± 1.6	28.1 ± 1.9	-

3.2. Zeta potential measurement

For many solid-liquid interaction studies, electrokinetic properties *i.e.* zeta-potential is an important surface property. Since this allows tuning or controlling the deposition of (bio)-macromolecules like proteins or cells. The zeta-potential (ζ) as a function of pH for the uncoated and PDMS coated microscope glass slides are shown in Fig. 2. Highly negative values are observed at neutral pH for piranha cleaned glass slides where a plateau is reached between pH 7 to 9.7. This ζ -potential values can be attributed to the presence of surface silanol groups and adsorbed hydroxyl ions.³² In comparison, PDMS shows a plateau in negative zeta-potential ($\zeta = -43$ mV) above pH 6. Also in this case the observed zeta-potential can be explained by

adsorbed ions. It should be noted that the zeta-potential is a direct measure of the charge density at the shear plane of the interface. Therefore, adsorbed ions have a strong influence on the measured values. The values presented in this work are comparable with data reported for PDMS bulk material.³³

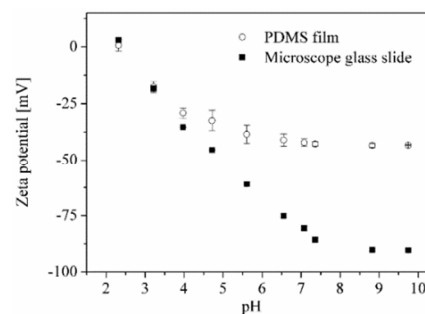


Fig. 2 Zetapotential of a microscope glass slide (solid squares) and PDMS (0.5 %, w/w) coated slide (closed circles) measured as a function of pH in 1 mM KCl.

3.3. Surface morphology

The optical microscope images (50-fold magnification) of films coated from 0.1–0.7 % (w/w) are shown in Fig. 3. A smooth and uniform distribution of PDMS can be seen for films manufactured at concentrations from 0.1 to 0.5 %. Whereas, at 0.7 % a more heterogeneous morphology with larger particles is detected. Such a feature can arise from the high viscosity of the solution which can hinder homogeneous film formation.

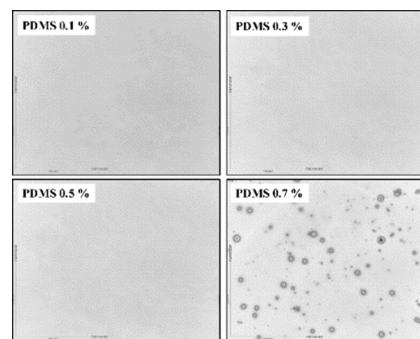


Fig. 3 Optical microscopy images (200 x 200 μm²) of PDMS thin films coated on silicon substrate at different concentrations (w/w).

Atomic force microscope (AFM) height images of surfaces of PDMS thin films coated onto gold substrates are depicted in Fig. 4. For comparison an uncoated QCM-D gold surface is included. PDMS coated surfaces prepared from 0.1 – 0.5 % (w/w) show smooth and flat features with a low root mean square roughness. A successful coating of PDMS and uniform surface coverage is

visible already at low concentration (0.1 %, w/w). Surfaces prepared from 0.7 % (w/w) were too inhomogeneous to give proper AFM results and were therefore not included in Fig. 4. The AFM data is in good agreement with the results obtained from optical (Fig. 3) and scanning electron microscopy (ESI, Fig. S4†) where smooth coatings of PDMS are observed up to a PDMS concentration of 0.5 % (w/w).

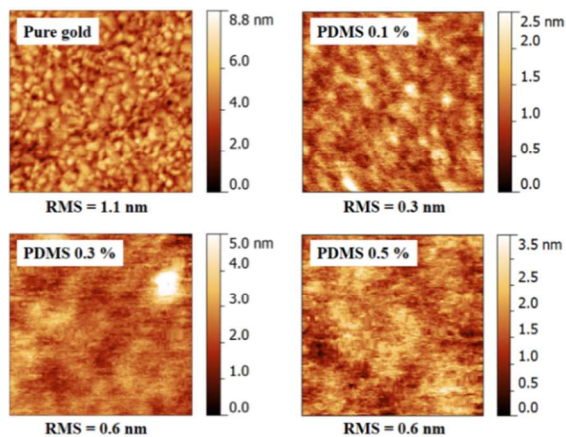


Fig. 4 Atomic force microscopy height images ($1 \times 1 \mu\text{m}^2$) of a gold substrate and PDMS coated surfaces. All concentrations are given in w/w.

For comparative reasons PDMS films were also successfully prepared from toluene on silicon wafers and from THF on gold substrates and silicon wafers. The AFM images of these films are shown in ESI† (Fig. S5-S7).

3.4. Surface wettability

The surface free energy (SFE) of the PMDS thin films was determined from the contact angle values of four test liquids. In contrast to uncoated silicon wafers ($\text{CA}(\text{H}_2\text{O}) = 19 \pm 1^\circ$), the PDMS coated surfaces from all concentrations exhibited a higher water contact angle *i.e.* between 105 and 111° .^{5, 34} The increase in contact angle is also observed for the other test liquids (see ESI, Table 1†). The calculated total SFE (γ_s^{TOT}) ranges from 19 to 12 mJ m^{-2} as the concentration increases, implying that PMDS can be regarded as a low energy surface with a dominant dispersive Lifshitz–van der Waals contribution (γ_s^{LW}). A low value of electron donating contribution (γ_s^-) is observable, which could originate from cross-linking agent or from surface impurities and adsorbed water. In general, the calculated $\text{CA}(\text{H}_2\text{O})$ and γ_s^{TOT} are typical for PDMS surfaces and correlate well with the published data.³⁵

Since surface topography and roughness play an important role in wetting of liquid droplets on solid substrates, advancing and receding contact angles were measured on PDMS and cellulose coated surfaces. All measured values are given in Table 2 of ESI†. For PDMS films manufactured from 0.1 to 0.5 % (w/w) the contact angle hysteresis is below 20° indicating relatively smooth and homogeneous films. Films manufactured from 0.7 % (w/w) are more

heterogeneous and therefore exhibit a contact angle hysteresis of 35° . This supports the data from optical imaging and SEM.

Furthermore, the $\text{CA}(\text{H}_2\text{O})$ was determined for the PMDS thin films (0.5 %, w/w) that were subjected to zeta-potential measurements (see section 3.2) and no significant change in water contact angle is observed even though the film was exposed to acidic and basic pH values. This experiments clearly evidence that the films are highly stable under these conditions and no delamination from the base glass substrates occurred. This was also confirmed by extensive stability measurements with QCM-D (ESI, Fig. S3†)

3.5. Spatial structuring of PDMS surfaces with cellulose/TMSC coatings

To extend the potential applicability of PDMS thin films we developed two simple surface structuring methods (scheme 1) that allow tailoring the hydrophobic PDMS surface with functional coatings of hydrophilic cellulose. Figure 5A shows TRITC stained pads of cellulose surrounded by TMSC on PDMS that were obtained by method 1. As expected only areas not protected by the metal mask were converted into pure cellulose. This was proven by fluorescence measurements where TRITC specifically binds to cellulose and not to TMSC (Fig. 5A).²⁶ Upon contact with HCl vapors, the trimethylsilyl (TMS) groups are cleaved off by acid-catalyzed process leading to pure cellulose.^{23, 24} This process allows constructing geometrically well-defined hydrophilic cellulose pads surrounded by hydrophobic TMSC. The successful conversion of TMSC into pure cellulose was further confirmed by water contact angle and layer thickness measurements. Thus, this structuring method allows to manufacture surfaces that can be selectively labeled with reactive compounds. The regenerated cellulose showed water contact angles of $32 \pm 1^\circ$ and layer thickness of $22 \pm 0.6 \text{ nm}$ in contrast to TMSC (water contact angle = $99 \pm 1^\circ$ and layer thickness = $58 \pm 0.7 \text{ nm}$). The reduced water contact angle and layer thickness is a proof that hydrophobic TMSC is converted into hydrophilic pure cellulose as described by other authors.^{23, 24} Since our aim was to functionalize PDMS surfaces with hydrophilic cellulose, the coatings of cellulose/TMSC from Fig. 5A were rinsed with toluene in order to remove the TMSC without detaching the cellulose pads. These coatings are shown in Fig. 5B. The visible differences in the fluorescence intensity compared to Fig. 5A are due to the removal of excess reversibly bound dyes during the rinsing step. To verify the complete removal of TMSC, the coatings from Fig. 5B were exposed to hydrochloric acid vapors without applying a mask and subsequently stained with TRITC. In this case, the same results as in Fig. 5B were obtained confirming the absence of cellulose. However, upon exposure of coatings shown in Fig. 5A to hydrochloric acid vapors, conversion of the non-regenerated TMSC into pure cellulose could be observed (Fig. 5C). In addition, water contact angles were measured at the places where TMSC coatings were rinsed with toluene and exposed to hydrochloric acid vapors. A high water contact angle (110°), similar to the value observed for pure PDMS coated surfaces, was detected. From the results above, it can be concluded that the TMSC coatings are removed from the PDMS surface. Furthermore, it can be observed that much lower amounts of TRITC are bound to the PDMS surface. Altogether this

method provides the opportunity to fabricate patterned PDMS surface by controlling the dimension of cellulose pads and by choosing a defined mask.

In method 2, patterns of cellulose on PDMS surfaces were obtained by a two-step process: UV/ozone treatment followed by spray coating of TMSC and subsequent regeneration into cellulose. UV/ozone treatment of PDMS surfaces that produces SiO_x is essential in order to enhance the adhesion of TMSC layers to the surface. Successful activation of PDMS upon UV-exposure and conversion of TMSC into cellulose was investigated with film thickness, contact angle and fluorescence measurements. The contact angle measurement showed that the water wettability of the UV/ozone treated surfaces decreased drastically from contact angles of $111 \pm 1^\circ$ to $25 \pm 0.4^\circ$, confirming the conversion of PDMS into hydrophilic SiO_x.³¹ As can be seen from QCM-D measurements (ESI, Fig. S2†), a 10% reduction in film mass is observed, suggesting that UV/ozone treatment does not completely remove the coatings, but modifies it into SiO_x.^{16, 31} The regeneration of TMSC into cellulose is clearly visible from the fluorescence signal as a result of TRITC binding (Fig. 5D). However, compared to spin coated cellulose a high fluorescence signal is observed for spray coatings. Spray coating leads to thicker (41 ± 2.3 nm) and rougher layers which can bind higher amounts of dye.³⁶ The stability of the developed patterns from both methods was additionally examined by rinsing with different buffer solutions (pH 3-9). It turned out that the developed structures are highly stable and do not detach from the PDMS surface. The developed patterned coatings are transparent and stable also in several apolar organic solvents. The geometry and wettability of the exposed areas can be precisely tuned by choosing a well-defined mask and by controlling the activation time. Using this approach a large variety of functional soluble polymers can be patterned spatially by simple spray coating and further functionalized with target moieties.

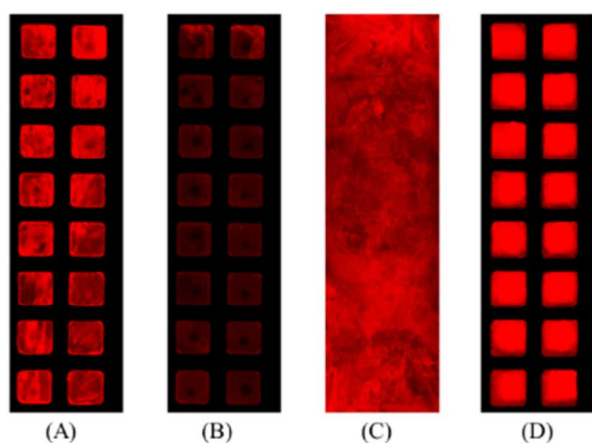


Fig. 5 Structured PDMS slides with cellulose/TMSC coatings, stained with TRITC. (A) Cellulose pads surrounded by TMSC. (B) Cellulose pads from structure A after removing TMSC by rinsing with toluene. (C) Fully cellulose coated PDMS. (D) Spray coated cellulose pads.

The surface morphology of cellulose pads coated on PDMS is shown in Fig. 6. Compared to the flatter and featureless PDMS (Fig. 4), a particle-like structure with a root means square roughness of 2.5 nm for spin coated and 4.9 nm for spray coated cellulose is noticeable. Cellulose surfaces show lower advancing /receding contact angles and a higher water contact angle hysteresis (see Table 2, ESI†) which can be attributed to higher surface roughness and a hydrophilic surface chemistry. This data in combination with fluorescence measurements support that PDMS is successfully functionalized with cellulose.

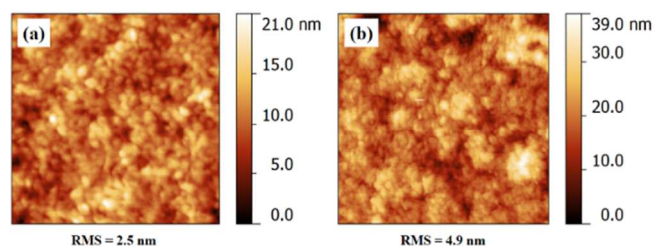


Fig. 6 Atomic force microscope height images ($1 \times 1 \mu\text{m}^2$) of a spin coated (a) and spray coated (b) cellulose surface on PDMS.

4. Conclusions

Thin films of PDMS with a thickness from 3 to 20 nm were manufactured and characterized in detail using several surface sensitive analytical methods. Spin coating of PDMS was successfully applied to obtain nanometric thin films on a wide range of substrates with good reproducibility from different solvents. The mass and film thickness increased linearly with the PDMS concentration. A highly negative zeta potential of -43 mV was determined for the PDMS films. Such films are smooth and stable under different pH environments. PDMS exhibits a high water contact angle, low surface free energy and a high dispersive Lifshitz–van der Waals contribution. Functionalization of PDMS thin films was conducted by depositing patterned hydrophilic cellulose by two different lithographic techniques. Cellulose pads surrounded by TMSC could be created by spin coating and spatial regeneration. The TMSC layers were selectively removed without detaching the cellulose pads by rinsing with toluene. The structures manufactured using the combination of UV/ozone etching and spray coating also resulted in the development of spatially separated cellulose. The developed protocols can be potentially extended to other, structurally similar polymers. It is further known that cellulose has a high binding affinity to water soluble antimicrobial chitosan and anti-adhesive carboxymethyl cellulose (CMC). The coating of these materials on the patterned cellulose surface can be of further interest for studies related to cell culture and for the development and analysis of antimicrobial and antifouling surfaces.

Acknowledgements

The financial support of Savatech d.o.o., Industrial rubber products and tyres is gratefully acknowledged. Prof. Volker Ribitsch from University of Graz, Austria is highly acknowledged for his help concerning zeta potential measurements. The authors are highly grateful to Dr. Aleš Doliška from University of Maribor and Mr. Florian Mostegel from the University of Leoben, Austria for AFM measurements. We also acknowledge B.Sc. Lucija Čoga and M.Sc. Luka Cmok from University of Ljubljana, Faculty of Mathematics and Physics, Slovenia for their support in Ellipsometry measurements and the CENN Nanocenter for the use of Accurion Nanofilm EP3 Ellipsometer.

Notes and references

^a Institute for the Engineering and Design of Materials, University of Maribor, Smetanova 17, 2000 Maribor, Slovenia. E-mail: mattej.bracic@gmail.com; Tel: +386-2-220-7898

^b Institute for Chemistry and Technology of Materials, Graz University of Technology, Stremayrgasse 9, 8010 Graz, Austria. E-mail: tamilselvan.mohan@uni-graz.at; Tel: +43-316-380-5413

^c Chair of Chemistry of Polymeric Materials, University of Leoben, Otto-Glöckel-Straße 2, A-8700 Leoben, Austria.

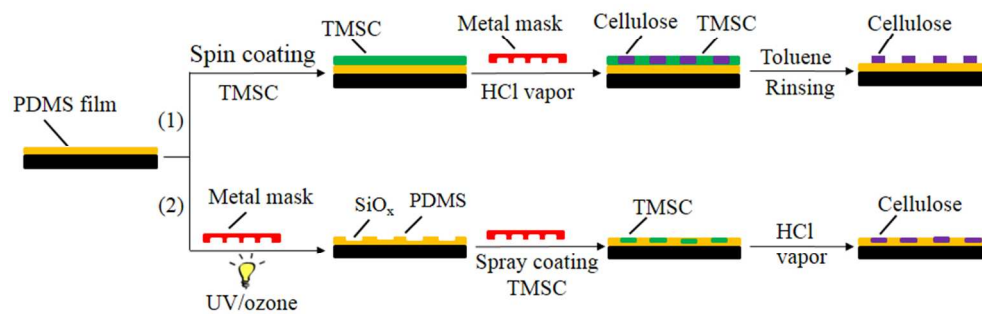
^dJoanneum Research Materials, Institute for Surface Technologies and Photonics, Franz-Pichlerstrasse 30, 8160 Weiz, Austria

^eSavatech d.o.o. Industrial Rubber Products and Tyres, Škofjeloška cesta 6, 4000 Kranj, Slovenia

† Footnotes should appear here. These might include comments relevant to but not central to the matter under discussion, limited experimental and spectral data, and crystallographic data.

Electronic Supplementary Information (ESI) available: [details of any supplementary information available should be included here]. See DOI: 10.1039/b000000x/

- J. C. McDonald, D. C. Duffy, J. R. Anderson, D. T. Chiu, H. Wu, O. J. A. Schueller and G. M. Whitesides, *ELECTROPHORESIS*, 2000, **21**, 27-40.
- Y. Xia and G. M. Whitesides, *Angewandte Chemie International Edition*, 1998, **37**, 550-575.
- Y. Xia and G. M. Whitesides, *Annual Review of Materials Science*, 1998, **28**, 153-184.
- J. H. Koschwaner, R. H. Carlson and D. R. Meldrum, *PLoS ONE*, 2009, **4**, e4572.
- K. Y. Chumbimuni-Torres, R. E. Coronado, A. M. Mfuh, C. Castro-Guerrero, M. F. Silva, G. R. Negrete, R. Bizios and C. D. Garcia, *RSC Advances*, 2011, **1**, 706-714.
- S. Grilli, V. Vespini and P. Ferraro, *Langmuir*, 2008, **24**, 13262-13265.
- K. Nakata, H. Kimura, M. Sakai, T. Ochiai, H. Sakai, T. Murakami, M. Abe and A. Fujishima, *ACS Applied Materials & Interfaces*, 2010, **2**, 2485-2488.
- D. Borah, S. Rasappa, R. Sentharamaikkannan, J. D. Holmes and M. A. Morris, *Langmuir*, 2013, **29**, 8959-8968.
- W. R. Childs and R. G. Nuzzo, *Langmuir*, 2004, **21**, 195-202.
- H.-L. Gou, J.-J. Xu, X.-H. Xia and H.-Y. Chen, *ACS Applied Materials & Interfaces*, 2010, **2**, 1324-1330.
- W. Chen, R. H. W. Lam and J. Fu, *Lab on a Chip*, 2012, **12**, 391-395.
- Y.-J. Fu, H.-z. Qui, K.-S. Liao, S. J. Lue, C.-C. Hu, K.-R. Lee and J.-Y. Lai, *Langmuir*, 2009, **26**, 4392-4399.
- J. Li, S. Ji, G. Zhang and H. Guo, *Langmuir*, 2013, **29**, 8093-8102.
- A. L. Cordeiro, S. Zschoche, A. Janke, M. Nitschke and C. Werner, *Langmuir*, 2009, **25**, 1509-1517.
- W. R. Childs, M. J. Motala, K. J. Lee and R. G. Nuzzo, *Langmuir*, 2005, **21**, 10096-10105.
- L. J. Matienzo and F. D. Egitto, *J Mater Sci*, 2006, **41**, 6374-6384.
- A. Oláh, H. Hillborg and G. J. Vancso, *Applied Surface Science*, 2005, **239**, 410-423.
- J. Zhou, A. V. Ellis and N. H. Voelcker, *ELECTROPHORESIS*, 2010, **31**, 2-16.
- Jeong Wong and C.-M. Ho, *Microfluid Nanofluidics*, 2009, **7**.
- D. Klemm, B. Heublein, H.-P. Fink and A. Bohn, *Angewandte Chemie International Edition*, 2005, **44**, 3358-3393.
- M. Tanaka, A. P. Wong, F. Rehfeldt, M. Tutus and S. Kaufmann, *Journal of the American Chemical Society*, 2004, **126**, 3257-3260.
- H. Zou, Q. Luo and D. Zhou, *Journal of Biochemical and Biophysical Methods*, 2001, **49**, 199-240.
- T. Mohan, R. Kargl, A. Doliška, A. Vesel, S. Köstler, V. Ribitsch and K. Stana-Kleinschek, *Journal of Colloid and Interface Science*, 2011, **358**, 604-610.
- E. Kontturi, P. C. Thüne and J. W. Niemantsverdriet, *Langmuir*, 2003, **19**, 5735-5741.
- S. Köhler, T. Liebert and T. Heinze, *Journal of Polymer Science Part A: Polymer Chemistry*, 2008, **46**, 4070-4080.
- R. Kargl, T. Mohan, S. Köstler, S. Spirk, A. Doliška, K. Stana-Kleinschek and V. Ribitsch, *Advanced Functional Materials*, 2013, **23**, 308-315.
- T. Mohan, T. Ristic, R. Kargl, A. Doliska, S. Kostler, V. Ribitsch, J. Marn, S. Spirk and K. Stana-Kleinschek, *Chemical Communications*, 2013, **49**, 11530-11532.
- A. Blau, T. Neumann, C. Ziegler and F. Benfenati, *J Biosci*, 2009, **34**, 59-69.
- M. M. B. Nielsen, *University of Southern Denmark*, 2012.
- M. Reischl, S. Kostler, G. Kellner, K. Stana-Kleinschek and V. Ribitsch, *Review of Scientific Instruments*, 2008, **79**, 113902-113906.
- F. D. Egitto and L. J. Matienzo, *J Mater Sci*, 2006, **41**, 6362-6373.
- S. Spirk, H. M. Ehmman, R. Kargl, N. Hurkes, M. Reischl, J. Novak, R. Resel, M. Wu, R. Pietschnig and V. Ribitsch, *ACS Applied Materials & Interfaces*, 2010, **2**, 2956-2962.
- B. Wang, R. D. Oleschuk and J. H. Horton, *Langmuir*, 2005, **21**, 1290-1298.
- E. T. de Givenchy, S. Amigoni, C. d. Martin, G. Andrada, L. Caillier, S. Gëribaldi and F. d. r. Guittard, *Langmuir*, 2009, **25**, 6448-6453.
- M. K. Chaudhury, *Journal of Adhesion Science and Technology*, 1993, **7**, 669-675.
- K. Norrman, A. Ghanbari-Siahkhalil and N. B. Larsen, *Annual Reports Section "C" (Physical Chemistry)*, 2005, **101**, 174-201.



Patterned Surface functionalization of PDMS with biopolymer cellulose via lithographic methods
254x190mm (96 x 96 DPI)